The Engineering Society
For Advancing Mobility
Land Sea Air and Space

400 COMMONWEALTH DRIVE WARRENDALE, PA 15096

SAE Technical Paper Series

870168

Heat Transfer in the End Gas

David P. Hoult, D. Hamiroune, and James C. Keck

Department of Mechanical Engineering

Massachusetts Institute of Technology

Cambridge, MA

International Congress and Exposition
Detroit, Michigan
February 23-27, 1987

All SAE papers are abstracted and indexed in the SAE Global Mobility Database

ISSN 0148-7191

870168

Heat Transfer in the End Gas

David P. Hoult,
D. Hamiroune,
and James C. Keck
Department of Mechanical Engineering
Massachusetts Institute of Technology
Cambridge, MA

ABSTRACT

This paper describes experimental and theoritical studies of a turbulent combustion bomb. We find a correlation between heat transfer to the wall and the initial turbulence intensity.

Wall temperature and pressure measurements were made for three levels of initial turbulence. All tests were performed with an equivalence ratio of 1.0, and the turbulence intensity was controlled by varying the time delay between mixture intake and spark ignition.

Assuming one-dimensional conduction, the surface heat flux was computed from the wall temperature data. Gas temperatures were computed from the pressure data assuming isentropic compression. Based on turbulent velocity measurements made in previous studies, these results permitted a correlation of Nusselt number with turbulent Reynolds number.

Using this correlation, we estimate the heat transfer in the end gas and its effect on the gas temperature. We use a chemical kinetic model to estimate the effect of the end gas heat transfer on the octane number required to prevent knock.

NOMENCLATURE

- $A(t)$ - area of the control volume
- c - specific heat of the wall (Btu/lbm.F)
- δ - boundary layer thickness
- h - the height of the bomb
- k - conductivity of the wall (Btu/hr.ft..F)
- K_3 - equilibrium constant
- m_o - initial mass of the gas in the bomb
- Nu - Nusselt number
- ν - kinematic viscosity
- O_N - octane number
- P - bomb pressure
- P_o - initial bomb pressure
- P_H - hydroperoxide mole number
- q_w - heat flux through the wall (Btu/ft^2-sec)
- Re_b - base flow Reynolds number
- Re_t - turbulent Reynolds number
- R - bomb radius
- R_o - inlet throat radius
- r - radial position of the particle
- r_o - position of a particle which arrives at the flame front at time t_o
- r_f - flame position
- ρ_u - unburned gas density
- ρ_b - burned gas density
- ρ_o - initial gas density
- S_b - burning speed
- S_L - laminar flame speed
- Tad - adiabatic gas temperature
- T_w - wall temperature
- T^* - elapsed time (t - total decay time)
- τ's - the characteristic reaction times
- U_r - mean speed of particle's motion
- U_b - base flow
- U_o - inlet throat velocity
- U_o' - initial turbulent intensity
- U_t - turbulent intensity
- V - vertical velocity due to the base flow boundary layer
- V_A - active valence mole number
- X_b - mass fraction burned
- Z - shifted turbulent time

0148-7191/87/0223-0168$02.50

WHEN THE WRINKLED FLAME PROPAGATES through the combustion chamber of a spark ignition engine, the gas ahead of the flame is compressed, and a motion is induced which is away from the flame front. The heat loss in the gas ahead of the flame, the "end gas", is of course not as large as the heat lost in the gas behind the flame as there the gas temperature is much higher, and hence the temperature difference driving the heat transfer much larger. But we shall show its importance in establishing whether knock will occur in the end gas.

In this paper we report on preliminary measurements of the end gas heat transfer measured in the MIT turbulent closed volume combustion bomb [1] in which the local turbulent intensity at the start of the combustion process is known. Heat transfer is measured at several points and is correlated with the properties of the flow induced by the flame propagation. We believe that these measurements are the first to correlate local turbulence properties with local, instantaneous heat transfer in a closed volume combustion process.

The apparatus is described in Section 2, as are the important results of previous studies of flame propagation and theoretical models of the end gas turbulence.

Section 3 describes the correlation of the Nusselt number which the current model has generated. It is found that the Nusselt number correlates best with the local turbulence intensity. A theoretical reason is presented to support this result.

We believe that these results have a important influence on the knock process, as recent studies of the knock chemistry [2] suggest that temperature changes as small as a few degrees Kelvin in the end gas can make major differences in the whether the end gas knocks or not. In Section 4 we outline the heat loss model and apply it to the MIT combustion bomb. We find temperature depressions in the core of the end gas of a few degrees Kelvin.

In Section 5, we calculated, using the Keck and Hu model [2], the shift in required octane number to prevent knock as a function of turbulent intensity in the end gas. Although this model calculation is preliminary, it clearly indicates the sensitivity of knock to end gas turbulence.

EXPERIMENTAL APPARATUS AND PAST RESULTS (Sec.2)

The combustion bomb is a closed cylinder consisting of two identical flat circular stainless steel plates and a circular stainless steel ring bolted together. The height of the combustion chamber is 15.875 mm and the diameter is 204.8 mm. As shown in Figure 1, two quartz windows, which provide optical access to the bomb, are located on the top and bottom plates. At the top center and bottom center of the bomb the intake valves are mounted, see Fig.1. Twenty two equally spaced automotive poppet valves for exhaust are located around the perimeter of the bomb.

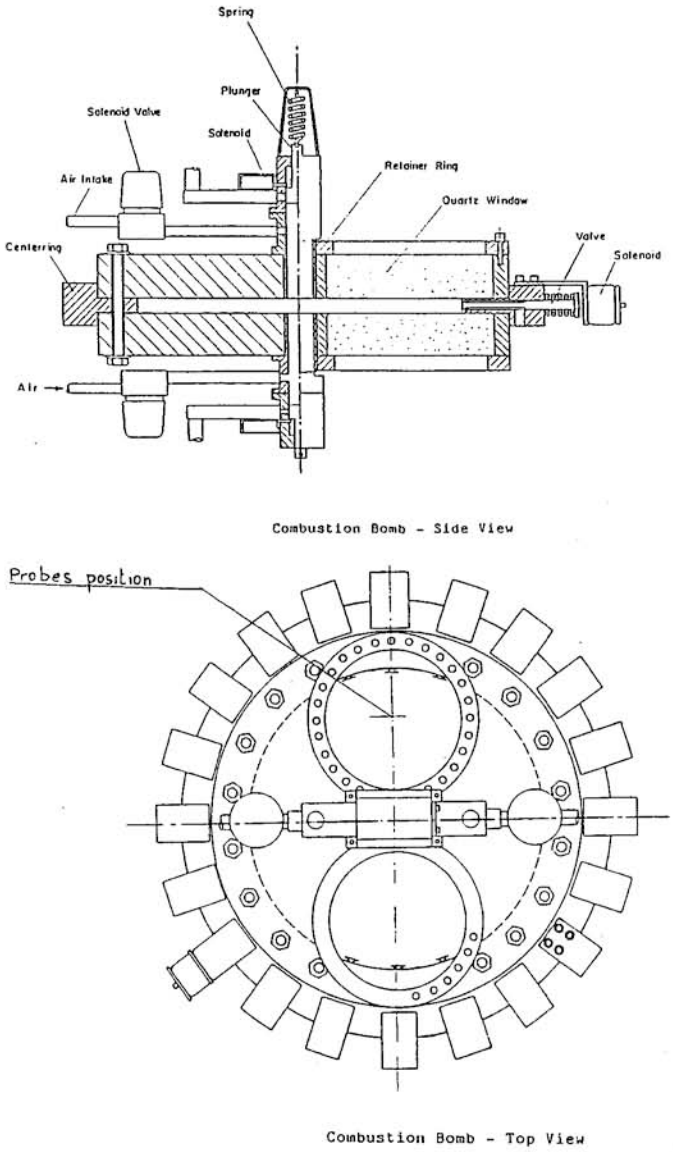

Figure 1. The Combustion Bomb, Top View and Side View

Figure 2 shows a cross section of the bomb. During the intake process, the flow is radially outward from the intake valves to the exhaust valves. Flow straighteners are suspended from the center of the bomb to insure that the turbulent flow is radially outward and has no separated regions. Reference [1] gives details on the apparatus and references on how the flow properties were determined.

In the heat transfer measurements reported here, one of the quartz windows is replaced with a steel plate in which are mounted pencil shaped "Eroding" type fast response thermocouples, manufactured by Nanmac. These probes are made of thin flat-ribbon thermocouples, which have a response time on the order of 0.01 ms. This characteristic time is much shorter than the time for a flame to propagate from the center to the outer radius of the chamber, about 30 ms.

It has been established by Hoult & Nguyen [1] that the flame shape in this bomb, as

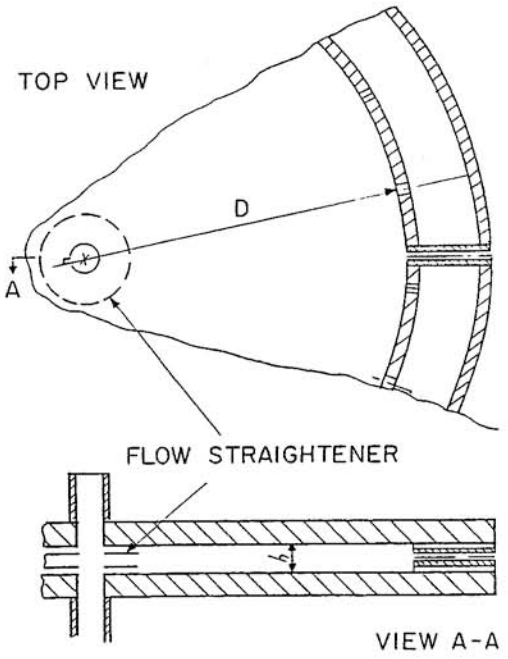

Figure 2a. Flow Straightener Mounted in the Bomb.

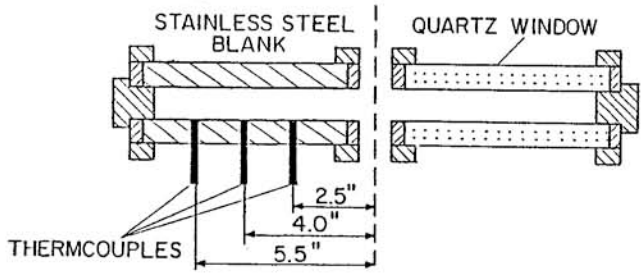

Figure 2b. Position of the Thermocouples.

observed through the quartz windows and recorded by Schlieren photography is approximately circular. Hence we shall use the flame radius as an indication of the flame position.

This simple pancake geometry has been studied theoretically using the Rapid Distortion Theory by Hoult & Wong [3] and Wong & Hoult [4]. An important construct of the theory is the base flow. The base flow is given by

$$\frac{1}{r}\frac{d}{dr}(rU_r) = -\frac{1}{\rho_u}\frac{d\rho_u}{dt} \qquad (1)$$

and the Lagrangian motion of a particle is given by

$$r(r,t|r_o,t_o) = \sqrt{\frac{\rho_a}{\rho_u} r_o^2 + R^2\left(1 - \frac{\rho_a}{\rho_u}\right)} \qquad (2)$$

Hoult and Nyguen [1] found that provided the initial state is turbulent enough, i.e. that

$$1.0 < U_o'/S_L < 3.0 , \qquad (3)$$

the position of the flame radius and the pressure rise scale the with the same time parameter

$$Z = \frac{T^* U_o'}{h} + \text{constant} \qquad (4a)$$

and the mass fraction burned is given by

$$X_b = \frac{P(t) - P_a}{P_{max} - P_o} \qquad (4b)$$

while the flame front is given by

$$\frac{r_f}{R_o} = 3.93 + 21.58\,Z - 30.82\,Z^2 + 18.09\,Z^3 . \qquad (4c)$$

In ref. [1] this scaling was shown to lead to a remarkable result: when the turbulence model is considered to be the random motion which remains after the base flow is subtracted out, a linear turbulence model is required to generate the scaling observed.

Although RDT is one such linear turbulence model, the sum of the indirect evidence is that the amplification predicted by the theory is not observed [see ref. [1].

Experimentally, the turbulent intensity is controlled by controlling the time the turbulence decays before the spark fires. Reference [5] reports the measurements of the decaying turbulence, once the valves are closed.

In developing the final heat transfer correlation, we use the Z scaling (eq. 4), and equation (2) to define the local turbulent intensity used in equations (9) and (10).

With this knowledge of the local turbulent intensity and flame propagation which occur in the bomb, we turn now to the reduction of the heat transfer measurements. It can be shown that if $T_w(t)$ is the wall temperature, then the heat transfer to the wall $q_w(t)$ satisfies

$$q_w = \sqrt{\frac{k\rho C}{\pi}} \int_o^t \frac{1}{(t-\bar{t})^{1/2}} \frac{dT_w(\bar{t})}{dt} d\bar{t} \quad . \qquad (5)$$

See for example references [6,7].

Figure 3 shows a typical raw data plot of temperature vs time and Figure 4 shows the resulting heat transfer as a function of Z. These data are heat transfer at a specific radius, for a range of times before, during and after the flame passes over the probe.

In the next section we develop a scaling law for the local heat transfer. It is worth contrasting this data with the older Woschni correlation [8], which used global results to infer heat transfer coefficients and with the results of Greif et al. [6], where the detailed flow geometry in the combustion chamber is unknown.

Study of the data indicates that the heat transfer in the burned gas is less than expected (see ref. [9]). This arises in Figures 3, 4 and

5 because we inadvertently mounted the thermocouples slightly below the surface of the combustion chamber. When the flame passes over the thermocouple, there is a region of unburned gas around the probe due to the probe location, which insulates the probe, lowering the heat transfer rate observed in the burned gas. In repeating the experiments with proper probe lcoation, we find the heat transfer in the end gas unchanged.

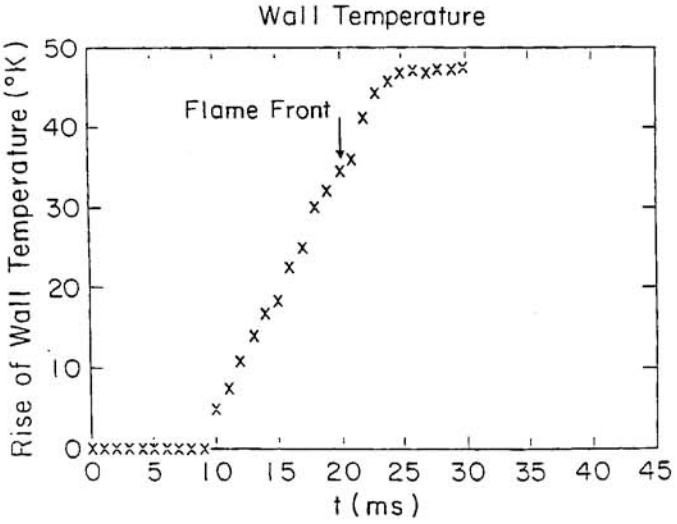

Figure 3. Wall Temperature Rise Function of Time.

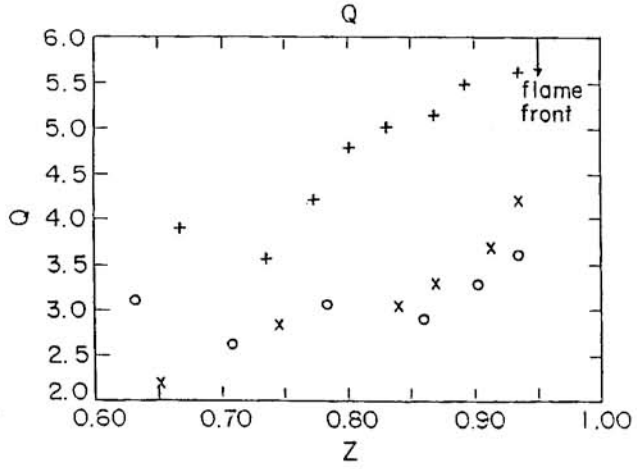

Figure 4. Heat Flux Through the Wall versus Z.

THE HEAT TRANSFER CORRELATION (Sec.3)

It is natural next to attempt to correlate the measurements of heat transfer, written as a Nusselt number,

$$Nu = \left(\frac{q_w}{T_{ad} - T_w}\right) \frac{l}{k} \quad , \qquad (6)$$

with a Reynolds number based upon the local base flow velocity, Eq. (1), i.e.

$$Re_b = \frac{U_b R}{\nu} \qquad (7)$$

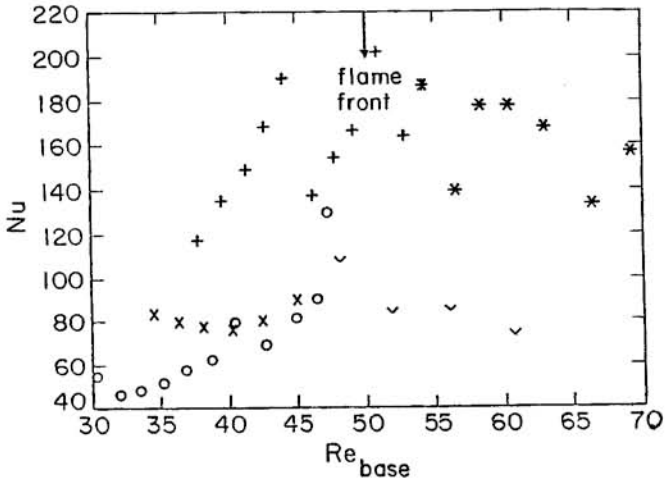

Figure 5. Nusselt Number versus Reynolds Number

This correlation is not successful. The reason is that the vertical velocity due to the base flow boundary layer, roughly

$$V = U_b \frac{d\delta}{dx} \approx 0.3 \ \text{(m/s)} \quad , \qquad (8)$$

is smaller than the initial turbulent intensity measured by Imohel [8] as the time of combustion and is much less than the turbulent intensity just outside the boundary layer.

$$U_t/V \approx 20.$$

Using the decay law determined by Imohel [8], we can calculate the turbulent intensity at the time combustion starts. For the definition of this time, see Ref. [1].

Next, we define a turbulent Reynolds Number as

$$Re = \frac{U_o' h}{\nu} \quad .$$

There is a rough correlation, shown in Figure 6.

However, this correlation uses an average turbulent intensity, typical of the whole bomb, at the time of the start of combustion. But at this time, it is known [5] that there is a substantial radial gradient in turbulent intensity and that, further, as the decay proceeds the radial gradient persists with the turbulence at each radius decaying at the same rate. Figure 7 from Ref. [1] shows this radial gradient function.

To correct the data for the gradient in turbulent intensity in principle requires local measurements of turbulent intensity ahead of the flame or a turbulence model to calculate the evolution of turbulent intensity with time. Lacking a convincing turbulence model and the data, we resort to a rough argument proposed by

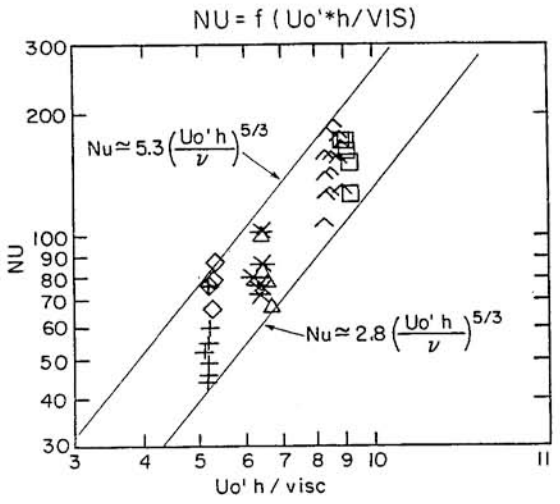

Figure 6. Nusselt Number versus Initial Turbulent Reynolds Number.

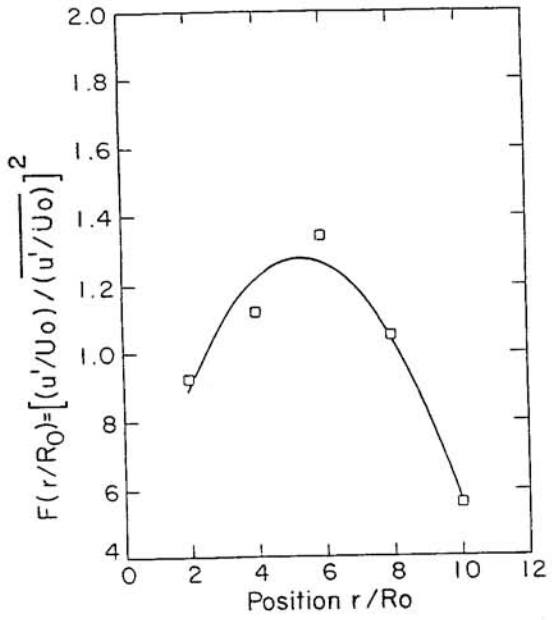

Figure 7. Radial Dependence of Turbulent Energy with Second Order Fit.

Hoult & Nguyen [1]: we assume that there is no amplification and that the turbulence is convected with the base flow as predicted by the Lagrangian equation (2). Of course, this estimate of the evolution of the turbulence in the end gas only crudely accounts for the intricate balance between rapid distortion and turbulent dissipation by assuming the two effects just balance.

We define a local turbulent Reynolds number as (see ref. [1], eq. 20):

$$U_t = U_o' \sqrt{F(r_o, t_o | r, t)/R_o} \quad , \qquad (9)$$

$$Re_t = \frac{U_t R}{\nu} \quad .$$

We next inquire if this Reynolds number produces an acceptable scaling of Nu. The resulting correlation, shown in Figure 8, is an improvement but scatter remains. Note the correlation has the form

$$Nu = 13.7 \ (Re_t^{1.17}) \quad . \qquad (10)$$

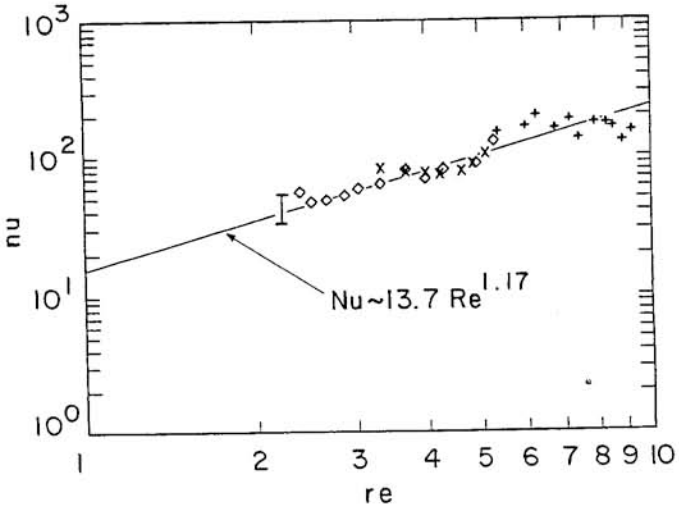

Figure 8. Nusselt Number versus Turbulent Reynolds Number.

Due to the linear property of the turbulence model which arises from the chosen base flow (see ref. [1]), the expected power of Re_t in this equation is 1.0. We expect that when a better estimate of the evolution of the turbulence becomes available, or when more detailed data of turbulent intensity ahead of the flame are well defined, the exponent will be closer to one.

Correlations of heat transfer with turbulence intensity outside the boundary layer have been observed previously at the stagnation point of bluff bodies and on a flat plate [see refs. 10, 11 and 12]. In all of these studies, correlations of a form similar to Eq. 10 are found.

THE HEAT BALANCE IN THE END GAS (Sec.4)

Consider the control volume shown in Figure 9. The inside boundary of the control volume, r(t), moves with the local base flow velocity, U_r. For simplicity, we assume that the heat and mass flux across this boundary are zero. Of

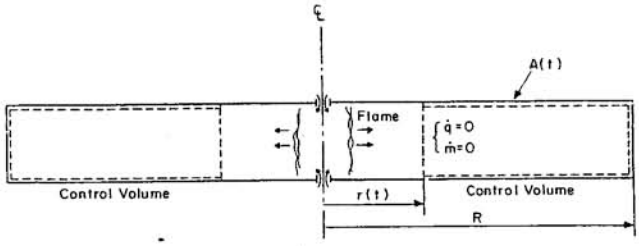

Figure 9. Cross Section of the Bomb Showing the Control Volume.

course, the mass flux across this boundary is zero only in the ensemble average and the heat flux is non zero. However, the temperature gradient across r(t) is much less than that from the core of the end gas to the cool wall, provided r(t) is chosen to be farther than one integral scale away from the flame front.

For the control volume chosen in this way, a first approximation to the decrease in bulk temperature of the end gas may be obtained by first law considerations, accounting for the heat loss through the walls of the control volume at

$$r(t)<r<R;\ z=+-h/2$$

and

$$-h/2<z<h/2;\ r=R.$$

For this control volume, the first law reduces to

$$dQ = m_o c_p \left(\frac{dT}{dt}\right) - m_o \left(\frac{RT}{P}\right) \left(\frac{dP}{dt}\right) \quad . \qquad (11)$$

The area of the cool walls of the control volume is

$$A(t) = 2 \frac{V_o}{h} \frac{P_o}{T_o} \frac{T(t)}{P(t)} + 2\pi Rh \quad . \qquad (12)$$

Equations 11 and 12 may be combined to yield a first order differential equation for T(t). Using the measured pressure history the bomb P(t) and an average heat transfer coefficient, the results shown in Figure 10 are found. In this figure, T_a is the adiabatic temperature of the end gas and DT is the estimated temperature decrease due to heat transfer. The temperature decrease is about 15 degrees Kelvin.

To understand how much the end gas temperature is lowered in an actual engine is clearly a formidable task, as it requires a detailed knowledge of the turbulent flow field

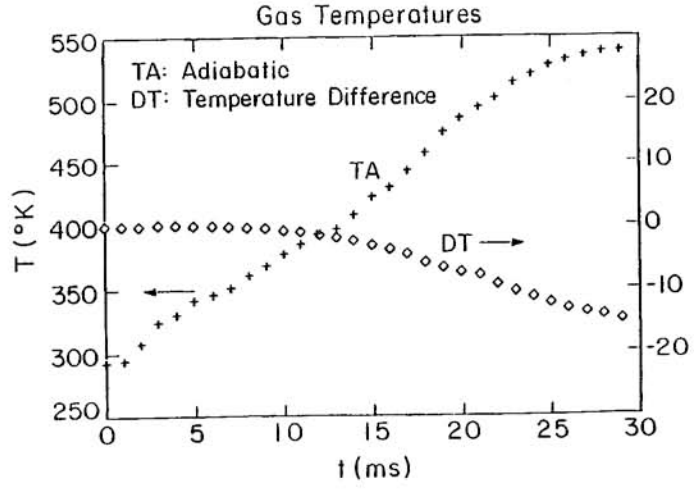

Figure 10. The Shift in Gas Temperature due to the Heat Flux in the Bomb.

at the start of combustion. However, we can make an estimate of the size of the effect with relatively little knowledge.

We consider a 90mm diameter cylinder in which the piston compresses a stoichiometric mixture 4 times and then remains at top dead center. The flame is assumed to be ignited on the centerline of the resulting pancake shaped combustion chamber. We estimate the pressure rise using the methods developed over many years [13]. A recent summary [14] describes the Blizzard and Keck model [15].

Using this methodology and a typical turbulent burning velocity, S_b, of 2m/s, the pressure rise can be computed by solving the coupled equations for flame position and mass fraction burned. The equation for mass fraction burned is (see eq. 7 of ref. [1])

$$m_o \frac{dX_b}{dt} = 2 \pi h \rho_u r_b S_b \quad , \qquad (13)$$

and the equation for flame position (see Eq. 9 of ref. [1]) is

$$\frac{dr_b}{dt} = S_b \cdot \frac{\rho_u/\rho_b}{1+[(\rho_u/\rho_b)-1).X_b]} \quad . \qquad (14)$$

With the resulting pressure - time history, we proceed to use the heat transfer correlation to calculate the decrease in end gas temperature as before. Figure 11 shows the decrease in end gas temperature for turbulent intensities from 1 to 5.5m/s. The decrease in end gas bulk temperature varies from a few degrees Kelvin to nearly 20 K.

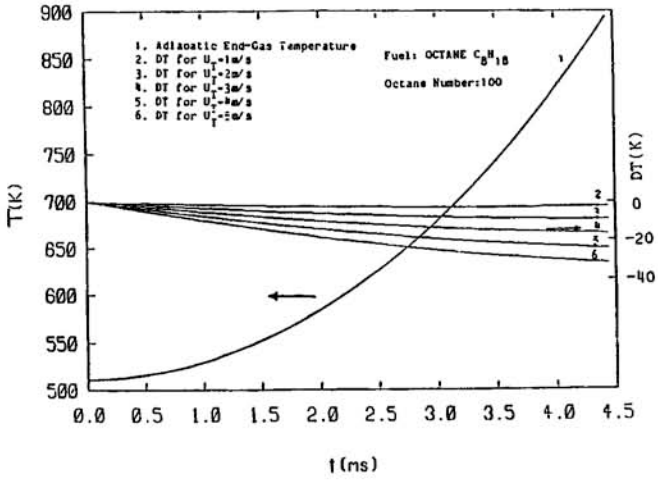

Figure 11. The effect of the Turbulent Intensity on the Gas Temperature.

Of course, holding the piston fixed ignores the relationship between the turbulent intensity and mean piston speed (u_t =1/2Up, see ref.[16]). Also, the effect of heat transfer is over stated

because, after TDC, the end gas is adiabatically expanded, and hence is a bit cooler, thus lowering the heat transfer rate.

KNOCK CALCULATIONS (Sec.5)

In this section, we use the recent chemical kinetic model of Keck and Hu [2] to estimate the effect of end gas heat transfer on the octane number required to just avoid knock. The purpose of the calculation is to access the role of turbulent heat transfer on octane requirements.

The Keck and Hu model is based on a branched chain model suggested by Benson [17] and is expected to be valid for simple alkanes with carbon numbers greater than four in the temperature range 600 to 750K. The model has been compared with experimental results from a constant volume bomb [2] and rapid compression machines [18] and [19] and good agreement has been obtained with minor adjustments in previously published rate constants. The Keck and Hu model may be contrasted with earlier, simpler knock calculations in which a single delay time was used [20] and with the similar Cox and Cole model [21] in which large adjustments in key rate constants were made.

The Keck and Hu model involves the pair of coupled rate equations

$$\frac{dV_A}{dt} = \frac{O_2}{\tau_1} + \frac{P_H}{\tau_7} \tag{15}$$

$$\frac{dP_H}{dt} = \frac{V_A}{\tau_c} - \frac{P_H}{\tau_7} \tag{16}$$

where V_A is the active valence mole number and P_H is the hydroperoxide mole number.

The characteristic reaction times τ_1 and τ_7 in these equations are given by

$$\tau_1 = (2k_1\,[RH])^{-1} \tag{17}$$

and

$$\tau_7 = k_7^{-1} \tag{18}$$

where k_1 is the rate constant for the initiation reaction

$$RH + O_2 \rightarrow \dot{R} + \dot{H}O_2 \tag{R1}$$

and k_7 is the rate constant for the branching hydroperoxide reaction

$$ROOH \rightarrow \dot{R}O + \dot{H}O \tag{R7}$$

In the temperature range specified, the characteristic cycle τ_c time for the chain which produces the ROOH is given by

$$\tau_c = (K_3 k_4\,[O_2])^{-1} \tag{19}$$

where K_3 is the equilibrium constant for the isomerization reaction

$$\dot{R}O_2 \rightarrow ROOH \tag{R3}$$

and k_4 is the rate constant for the association reaction

$$ROOH + O_2 \rightarrow \dot{O}OROOH \tag{R4}$$

The energy equation for the model is

$$\frac{d}{dt}\,\ell nT = \frac{\gamma-1}{\gamma}\,\frac{d}{dt}\,\ell np + \frac{Q_c}{C_p T}\,\frac{d}{dt}\,(P_H+V_A) \tag{20}$$

where Q_c is the chemical heat release per cycle, C_p is the heat capacity at constant pressure, and γ is the specific heat ratio. In the subsequent analysis we assume that the "knock" limit occurs when thermal effects due to the second term on the right hand side of Eq. 19 becomes of order 10^{-2} of the first term.

The required rate constants for the model are summarized in Reference [2] and are expected to be relatively insensitive to fuel structure and molecular weight. However the equilibrium constant K_3 is expected to depend on both these properties. For normal heptane, $K_3(H)$ has been estimated by Benson and gives results in satisfactory agreement with experiments. For isooctane, experiments indicate $K_3(I) \approx K_3(H)/3$. The octane scale is based on mixtures of these two primary reference fuels and experiments suggest that the effective equilibrium constant for such mixtures may be approximated

$$K_3(O_N) = K_3(H)(1 - .0067\,O_N) \tag{21}$$

where O_N is the octane number.

To assume the validity of the kinetic model, the compression ratio was adjusted in the calculations of Section IV until the end gas for isooctane fuel had a temperature less than 900K as the flame reached the outer edge of the combustion chamber. The flame speed used, 6 m/s, is a value quite consistent with experience [16].

For O_N = 100, and different turbulent intensity, Figure 12 shows the rise in peroxide as a function of time. There are two stages in the kinetic model. During the first stage $O_2/\tau_1 > P_H/\tau_7$ and V_A rises linearly with time while P_H rises quadratically. During the second stage $O_2/\tau_1 < P_H/\tau_7$ and both V_A and P_H rise exponentially. Appreciable heat release occurs only when the peroxide concentrations become larger than about $[O_2]/1000$. At this point, it is arbitrarily assumed that knock occurs. Notice how the knock point changes with the turbulent intensity. The exact value of the knock criteria makes little difference due to the very rapid rise in peroxide concentration after 5 ms.

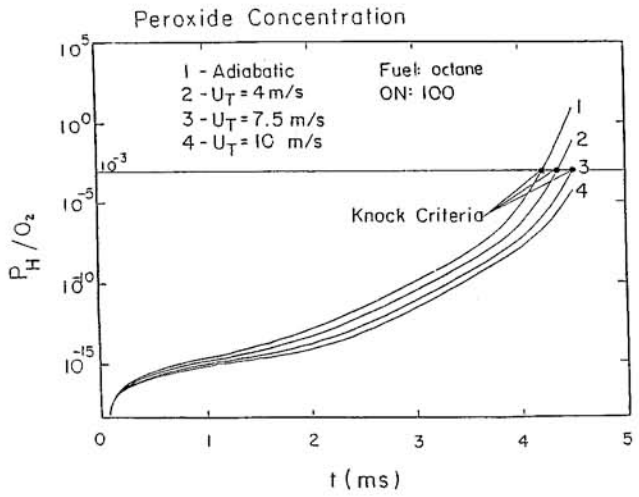

Figure 12. The Variation of the Ratio of the Peroxide and Oxygene Concentrations Function of Time.

Using this knock criteria and the depression in end gas temperature estimated due to heat transfer estimated in Section IV, we calculate the minimum required octane number to prevent knock as a function of end gas turbulent intensity. The variations in turbulent intensity, of course, change both flame speed and heat transfer. The result is shown in Figure 13. For large turbulent intensities, a very substantial decrease in required octane number occurs.

To estimate the region of practical turbulent intensities, we need to know the relationship between the turbulent burn velocity and the initial turbulent intensity. This requires simultaneous information on the initial turbulent intensity, the base flow ahead of the flame, and the burn velocity. Such data are available in ref. [1]: the observed velocity S_b is about 1.8 times the initial turbulent intensity [1].

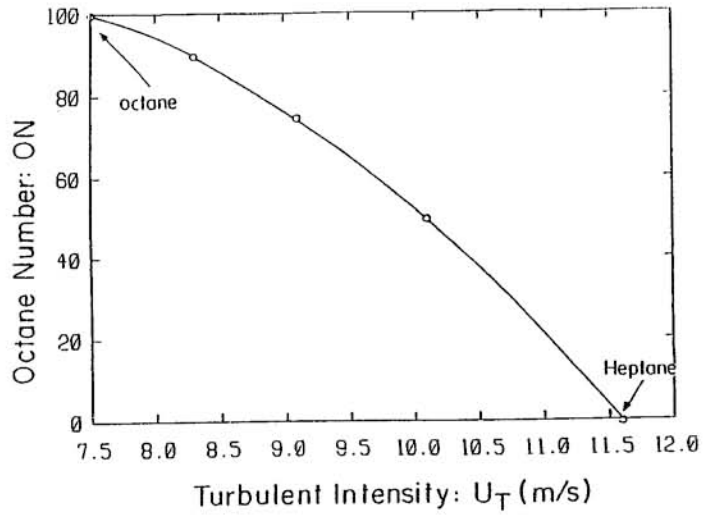

Figure 13. The Change of the Octane Number versus Turbulent Intensity.

In this range, the decrease in octane number with turbulent intensity is about -10 octane numbers per m/s increase in turbulent intensity. To extend the calculations to higher temperatures a kinetic model which includes reactions important in second stage hydrocarbon oxidation is needed. Work on this problem is in progress.

ACKNOWLEDGEMENT

This work is supported by the Department of Energy's Lean Engine Efficiency Program under contract number DE-AC04-81AL16310.

REFERENCES

1. D.H. Hoult and V.H. Nguyen, "A Turbulent Burning Law Derived From Combustion Experiments," JSME, SAEJ, MESJ International Symposium on Diagnostics and Modeling of Combustion in Reciprocating Engines Sept. 4-6, 1985.
2. J.C. Keck and H. Hu, "Explosions of Adiabatically Compressed Gases in A Constant Volume Bomb," Presented at the 21st International Symposium on Combustion, Munich, West Germany, August 1986.
3. D.P. Hoult and V.W. Wong, "The Generation of Turbulence In An Internal Combustion Engine," presented at 1978 GMR Symposium on Combustion Modeling in Reciprocating Engines, Warren, MI,November 6-7, 1978; Combustion Modeling in Reciprocating engines, Editors: J.N. Mattavi & C.A. Amann, pp. 131-155, Plenum Press (1980).
4. V.W. Wong and D.P. Hoult, "Rapid Distortion Theory Applied to Turbulent Combustion," SAE paper 790357, SAE Congress and Exposition, Detroit, MI, February 26 - March 2, 1979; SAE Transactions, Vol. 88 (1979).
5. W.J. Imoehl, "A Study of Turbulence Decay in A Turbulent Combustion Bomb," M.S. Thesis, Dept. of Mech. Engg., MIT 1985.
6. F.K. Tsou and S.J. Chen, "Measurements of Heat Transfer Rates Using a Transient Technique," ASME paper 83-HT-87 (1983).
7. R. Grief, T.Namba and M. Nikanhan, "Heat Transfer During Piston Compression including Side Wall and Convection Effects," Int. J. Heat Mass Transfer. Vol.22, pp.901-907, 1979.
8. G. Woschni, "A Universally Applicable Equation For the Instantaneous Heat Transfer Coefficient in the Internal Combustion Engine," SAE paper 670931, SAE Transactions, Vol. 77, 1967.
9. A.C. Alkidas and R.M. Cole, "Transient Heat-Flux Measurements in a Divided-Chamber Diesel Engine," ASME 84-HT-44.
10. M.C. Smith and A.M. Kuethe, "Effects of Turbulence on Laminar Skin Friction and Heat Transfer, " Phys. Fluids, 9, 2337(1966).
11. J. Kestin, "The Effects of Freestream Turbulence on Heat Rates," Advanced in Heat Transfer, Vol.3, Academic Press, New York, 1966, pp. 1-32.
12. T.R. Galloway, "Enhancement of Stagnation Flow Heat and Mass Transfer Through Interactions of Free Stream Turbulence," AICH9E Journal, Vol.19, p. 608 May, 1973.

13. J.A. Gatowski, E.N. Balles, K.M. Chen, F.E. Nelson, J.A. Ekchian and J.B. Heywood, "Heat Release Analysis off Engine Pressure Data," SAE Paper 841359, SAE International Fuels & Lubricants Meetings, October 8-11, 1984.
14. E.C. Bedran and G.P. Beretta, "General Thermodynamic Analysis for Engine Combustion Modeling," SAE Paper 850205, SAE International Congress & Exposition, Detroit, MI, February 25-March 1, 1985.
15. N.C. Blizard and J.C. Keck, "Experimental and Theoretical Investigation of a Turbulent Burning Model for Internal Combustion Engines," SAE paper 740191 SAE Automotive Engineering Congress, February 25 - March 1, 1974; SAE Transactions, Vol. 83 (1974).
16. J.B. Heywood, "Internal Combustion Engine Fundamentals," MIT February 1986, to be published.
17. S.W. Benson, Prog. Energy Combust. Sci. 7 125 (1981); see also Oxidation Communications 2 169, (1982).
18. C.F. Taylor, E.S. Taylor, J.C. Livingood, W.A. Russell and W.A. Leary, SAE Transactions 4 232 (1950).
19. H. Rogener and Z. Elektrochem 53 389 (1949)
20. A. By, B. Kempinski and J.M. Rife, "Knock in Spark Ignition Engines," SAE Paper 810147, SAE Congress and Exposition, Detroit, MI, February 23-27, 1981.
21. R. A. Cox and J.A. Cole, Combust. Flame 60 109 (1985).